J Solid State Electrochem (1999) 3: 258–263

ORIGINAL PAPER

S.S. Bhoga · K. Singh

A new Na^+ glass-dispersed Na_2CO_3 composite for a solid state electrochemical CO_2 gas sensor

Received: 12 June 1998 / Accepted: 21 October 1998

Abstract The electrical conductivity of the $40Na_2O$:$50SiO_2$:$10B_2O_3$ glass-dispersed Na_2CO_3 composite solid electrolyte system, prepared by liquid phase sintering, is systematically investigated using complex impedance spectroscopy. The unreacted glass glues the Na_2CO_3 grains together, which not only reduces the micropores but also improves the ionic conductivity and mechanical strength of the pellet. The conductivity enhancement in such a composite solid electrolyte system is discussed in the light of the increased concentration of charge carriers in a diffuse space charge layer formed at the crystalline-glass interface. A galvanic CO_2 gas sensor using an optimised composite electrolyte (50 wt% glass-dispersed Na_2CO_3) is found to be more stable against thermal cycles (heating and cooling) vis-à-vis the sensor based on a pure crystalline solid electrolyte.

Key words Solid electrolytes · Ionic conductivity · Sensor · Complex impedance · Interface

Introduction

Recently, there has been a strong incentive to engineer for electrochemical gas sensors those materials which are thermodynamically stable and exhibit appreciably high ionic conductivity. Polycrystalline ion conductors, rather than their single crystal counterparts, and glasses are preferred in such applications owing to certain advantages, especially the ease of fabrication into the required shape and size, isotropy in physical and mechanical properties, good response times and thermodynamic stability, etc. [1]. However, the greatest drawback associated with polycrystalline materials is the presence of in-built micropores, which hinder the mobility of ions. In addition to this, during the sensor operation at high temperatures with cooling and heating cycles, these materials develop micro-cracks, allowing permeation of the gas towards the reference; eventually this degrades the sensor [2]. On the other hand, in general, high ionic conducting glasses posses a low glass transition temperature (T_g) which restricts their use in sensors operating at moderately high or very high temperatures. Additionally, there is a major problem in achieving a good electrode (solid)-electrolyte (glass) interface contact. Interestingly, when the glass-dispersed crystalline samples are sintered just above T_g, the added glass passes into the molten state and flows across the grains, by capillary action, and fills the pores present therein. Such a process not only reduces the pores in the sample but also increases the mechanical strength and ionic conductivity [3].

In the recent past, development of CO_2 gas sensors has gained much of attention owing to their potential industrial applications. CO_2 is very difficult to detect by conventional gas sensors for the reason of its high stability at ambient temperatures. Most of the sensors reported earlier [4–6] have been required to be operated at a high temperature (973 K). In 1986, Maier et al. [7] for the first time constructed a CO_2 gas sensor using an open reference. Since then, many types of devices have been investigated using metal oxides [8], zeolites [9] and polymers with a carbonate solution [10]. The performance of these sensors, however, has not been satisfactory. Recently, sensors based on Na^+ conductors, β-alumina [11] and NASICON [12] coated with a Na_2CO_3 auxiliary electrode have been reported to respond well to changes in concentration. However, the response time has been several minutes at 773–973 K.

The selection of an apt carbonate-based material, as either a solid electrolyte or auxiliary electrode, has become crucial from sensitivity, response time, long term

S.S. Bhoga
Department of Physics, Nagpur University,
Nagpur-440010, India

K. Singh (✉)
Department of Physics, Amravati University,
Amravati-444602, India

stability and impervious to thermal shocks viewpoints. A detailed literature survey, however, reveals that, so far, much less attention has been paid towards the development of carbonate-based solid electrolytes. All the above factors have prompted us to develop a polycrystalline-glass composite solid electrolyte system for a CO_2 gas sensor. In this respect, a number of compositions belonging to Na^+ glass ($40Na_2O.50SiO_2.10B_2O_3$) dispersed Na_2CO_3 composite solid electrolyte system have been synthesised using the liquid phase sintering (LPS) technique. A few galvanic CO_2 sensors have been fabricated utilising an optimised composition and have been characterised.

Experimental

The $40Na_2O:50SiO_2:10B_2O_3$ glass (selected on the basis of the high Na^+ conductivity among the series) was prepared by melting together appropriate mole fractions of the initial ingredients Na_2CO_3, SiO_2 and B_2O_3 (with 99.99% purity procured from Aldrich, USA) followed by quenching in a stainless steel mould kept at room temperature [13]. The Na^+ glass obtained was crushed and sieved to get a fine powder of average particle size 2 μm. The Na_2CO_3 (finely ground) with 10, 20, 30, 40, 50 and 60 wt% of Na^+ glass was mixed thoroughly under acetone. Later, the homogeneously mixed powder of each composition was pressed uniaxially in a stainless steel die-punch at 3000 kg/cm^2 pressure so as to obtain a pellet of the dimensions approximately 1–2 mm in thickness and 9 mm in diameter. The pellets thus obtained were finally sintered at 20 K above the glass transition temperature (T_g = 698 K) for 1 h. The pellets of optimum conductivity at a given composition were sintered at different temperatures varying from 673 to 798 K for a fixed duration of 1 h so as to optimise the preparative parameter. The samples were characterised by X-ray powder diffraction using a Philips PW 1700 X-ray powder diffractometer (attached with PW 1710 controlling unit) using Cu-K α radiation, and the microstructures were observed using a Cambridge 250 mark-III scanning electron microscope.

Electrical conductivity measurements on samples stored for three months were carried out to ensure thermodynamic stability. A good ohmic contact was ensured by using sputtered gold film on both the flat surfaces. Prior to the impedance measurements, the spring-loaded samples were initially heated to 673 K and allowed to cool in steps of 20 K. During the cooling cycle (in the range from 673 to 473 K), the samples were maintained at each set temperature for 1 h (dwell time) so as to homogenise the charge carriers as well as to attain thermodynamic stability within them. The real and imaginary parts of the impedance were measured, at the end of each dwell time, as a function of frequency ranging from 5 to 13 MHz using a computer controlled HP 4192A LF impedance analyser as described earlier [14]. The reproducibility of the impedance data was confirmed by repeating the measurements on a new batch of samples. The ionic transport number of the samples was determined using Wagner's d.c. polarisation technique on the cell:

(+)Pt (rf sputtered film)/electrolyte/(metal) Na(−)

with the help of a Keithley 617 programmable electrometer as also described earlier [15].

A few electrochemical galvanic sensors with following configuration:

Na_2ZrO_3 + ZrO_3 (reference)/50glass:50 Na_2CO_3 (solid electrolyte)/rf sputtered gold film

were constructed employing the cold press technique, i.e., pelletising the reference and electrolytes separately and then stacking them together [16]. The sensor was characterised at 670 K. The test gases of pre-decided partial pressures (CO_2 in 21% O_2 and remaining Ar gas) were obtained using electronic mass flow meters-cum controllers (Teledyne Hestings, USA). The response time and reversibility of the sensor was tested by toggling the concentration of CO_2 between 1% and 500 ppm, and simultaneously recording the cell emf as a parametric function of time using the Keithley 617 programmable electrometer having an input impedance $\approx 10^{13}$ Ω. In order to test the effect of thermal cycling on the performance, the sensors with composition ($50glass:50Na_2CO_3$) and pure Na_2CO_3 as solid electrolytes, hereafter termed as S_c and S_p, respectively, were subjected to cooling and heating cycles between 298 and 723 K. At the end of each thermal cycle the emf of the sensors was measured as a parametric function of time at a fixed 500 ppm CO_2 partial pressure and 670 K temperature.

Results and discussion

The absence of peaks corresponding to crystalline Na_2O, SiO_2, B_2O_3 or intermediate new phases indicates the dispersion of unreacted Na glass into the crystalline Na_2CO_3 matrix [17]. The transference number measurements (Table 1) show a negligible electronic contribution, σ_e, to the total electrical conductivity, σ_T($\sigma_T = \sigma_i + \sigma_e$, where σ_i denotes conductivity due to ions), in the temperature range of the investigation.

Table 1 Electronic transport number and impedance data[a] for $(1-x)Na_2CO_3:(x)40Na_2O:50SiO_2:10B_2O_3$) glass composite electrolyte system at 673 K

Conc.	t_i	Low frequency semicircle				High frequency semicircle					
		R_{b1} (kΩ)	α_1	f_{p1} (kHz)	E'_a (eV)	R_{b2} (kΩ)	α_2	f_{p2} (kHz)	E''_a (eV)	S_{i1} (kΩ)	S_{i2} (kΩ)
x = 00	0.997	016.8	–	1574	0.820	012.7	–	2818	0.783	1.23	0.06
x = 10	0.998	015.6	0.88	1584	0.902	014.7	0.83	1995	0.857	1.93	0.07
x = 20	0.999	014.6	0.87	1412	0.938	014.4	0.80	2238	0.889	2.57	0.09
x = 30	0.999	004.8	0.88	4466	0.899	002.9	0.82	5623	0.855	1.07	0.08
x = 40	0.999	003.3	0.89	7079	0.894	003.1	0.85	11220	0.845	1.18	0.06
x = 50	0.999	–	–	–	–	003.0	0.85	10000	0.782	0.05	0.08
x = 60	0.999	003.4	–	7079	0.890	003.5	0.84	12589	0.856	1.75	0.07

[a] E'_a and E''_a calculated from $f_p = f_0 \exp(-E/kT)$, where f_0 is pre-exponential factor. S_{i1} and S_{i2} are standard deviations when one and two semicircles, respectively, are considered during non-linear least-squares fitting

The complex impedance plot for (70)Na_2CO_3:(30)Na glass at 673 K depicted in Fig. 1 reveals a distorted semicircular arc followed by an inclined straight line. An inclined straight line is attributed to the electrode-electrolyte interface [18]. On the other hand, the distorted semicircular arc is due to ion migration through the sample [18]. A close look at Fig. 1 suggests that the distorted semicircle is a combination of two overlapping depressed semicircular arcs. The non-linear least-squares fit (NLSF) method was used to ascertain the presence of two overlapping depressed semicircles and subsequent impedance analysis. In order to accomplish it, the complex impedance data acquired at a fixed temperature are fitted to following general equation:

$$Z(\omega) = Z(\infty) + \frac{Z(0) - Z(\infty)}{1 + (j\omega\tau^*)^{\alpha}} \quad (1)$$

where $Z(\infty)$ and $Z(0)$ are the limiting values of $Z(\omega)$, when the angular frequency ω changes to a maximum from zero, respectively; τ^* is the effective relaxation time and the α is related to the angle of depression. $\theta = \alpha\pi$. During NLS fitting the sum of squares is minimised by unity weighting:

$$S_i = \sqrt{[\Delta R_i)^2 + (\Delta I_i)^2]} \quad (2)$$

where ΔR_i and ΔI_i are real and imaginary fitting residuals, respectively. A similar technique has been used to ascertain the presence of two semicircles in the complex impedance plane [19]. The number of semicircles and other impedance parameters obtained at 673 K, following the above technique, are displayed in Table 1. As can be seen, except for the $(1-x)Na_2CO_3$:$(x)(40Na_2O{:}50SiO_2{:}10B_2O_3)$ glass composite, the deviation of the experimental points from the curve obtained from the NLSF is larger when one considers a single semicircle vis-à-vis two semicircles. Two overlapping depressed semicircular arcs in the complex impedance plane are suggestive of the occurrence of two prominent conduction mechanisms simultaneously under an external applied a.c. signal.

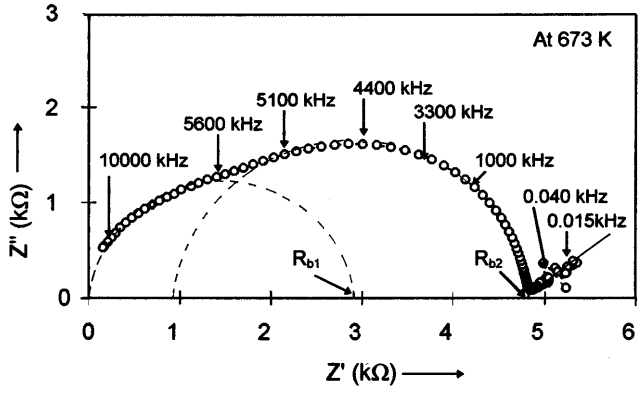

Fig. 1 Complex impedance plot for the $70Na_2CO_3{:}30(40Na_2O{:}50SiO_2{:}10B_2O_3)$ glass system, *dashed semicircles* are due to non-linear least-squares fitting and *points* are actual impedance data

The system under study is heterogeneous, i.e., there exists more or less abrupt structural changes. Heterogeneities encompass distinct interfaces between phases of unlike chemical composition. A redistribution of the ionic and electronic constituents takes place, so as to attain chemical and electrical equilibria, giving rise to a space charge region across the interface [20]. Various phases and junctions/interfaces contributing to the total conductivity of the present heterogeneous system are: (1) the Na glass, (2) the crystalline Na_2CO_3, (3) the homojunction (Na_2CO_3-Na_2CO_3 interface) and (4) the heterojunction (Na_2CO_3-Na^+ glass interface). In fact, the space charge regions are highly conducting, so they play critical roles in governing the electrophysical properties of the solids.

The transport of ions, leading to electrical conductivity, in each space charge region can be visualised as ions hopping from an occupied site to a nearby equivalent vacant one by traversing a barrier of height E_a. The barrier height is chiefly due to the electrostatic binding forces. The local environment, number of nearest-neighbouring atoms and inter-atomic distance as seen by the mobile ions in the space charge layers due to (1) crystalline-glass and (2) crystalline-crystalline interfaces differ considerably. Such a marked distinction in the local environment gives rise to the variation in the effective charge transfer activation energy barriers E'_a and E''_a (Table 1), corresponding to the crystal-crystal and glass-crystal interfaces, respectively, and thereby the difference in the relaxation times or the hopping frequencies (τ or f_p). Two semicircular arcs in the complex impedance plane are a reflection of the distinction in effective hopping frequencies. Maier [20] has also predicted two distinct hopping rates in the space charge regions due to homo- and hetero-junctions. A schematic representation of the composite electrolyte system along with its electrical equivalent circuit is depicted in Fig. 2. Here, the constant phase element (CPE) represents the distributed relaxation time that takes care of the depression in each semicircular arc. The hetero-junction is the highest conducting amongst all the above-mentioned phases and interfaces. Only one semicircle in optimum conductivity giving (50)(Na_2CO_3:(50)Na^+ glass composition (Table 1) is the manifestation of a percolation threshold wherein the space charge layer dominates [21].

The bulk conductivity of each sample (excluding the electrode-electrolyte interface effect) is obtained from complex impedance analysis. The plots of $\log(\sigma T)$ against $10^3/T$ for various compositions (Fig. 3) are seen to obey Arrhenius' law (Eq. 3) over the entire temperature range of the investigation.

$$\sigma T = (\sigma T)_0 \exp\left[-(E_\sigma/kT)\right] \quad (3)$$

where $(\sigma T)_0$ and E_σ are the conductivity pre-exponential factor and activation enthalpy, respectively and k and T are Boltzhmann's constant and the temperature (in K), respectively. The insert of Fig. 3 reveals that the conductivity of Na_2CO_3 increases with the addition of glass

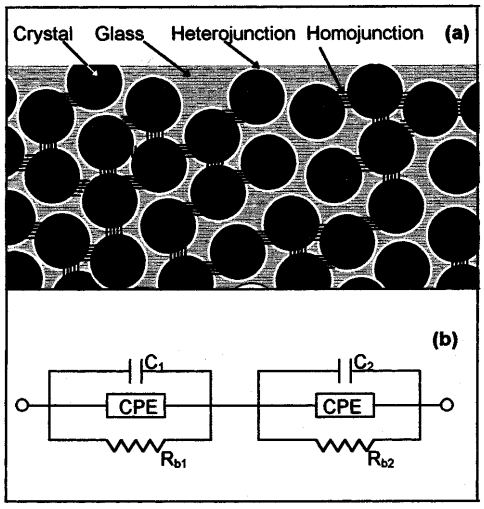

Fig. 2 a Schematic representation of Na_2CO_3:Na^+ glass composites and **b** electrical equivalent; R_{b1} and R_{b2} are due to homo- and hetero-junctions, respectively

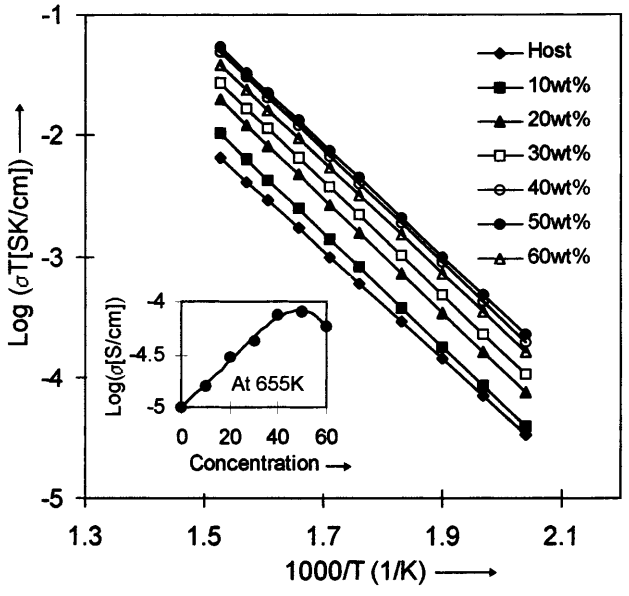

Fig. 3 Plots of $\log(\sigma T)$ versus $10^3/T$ for the Na_2CO_3:Na^+ glass composite system; *inset* shows a variation of $\log(\sigma)$ with glass concentration

up to 50 wt%, and decreases thereafter. The activation energy is seen to be lowest for the same composition (Table 1). As the concentration of glass in the Na_2CO_3 matrix increases, the total conductivity enhances due to: (1) a positive contribution from the high conducting glassy phase and (2) the formation of highly conducting pathways across the crystalline-glass interface (space charge layer) as shown in Fig. 2a. The maximum conductivity with the lowest activation energy for the $50Na_2CO_3$:$50[40Na_2O$:$50SiO_2$:$10B_2O_3]$ composition is due to the percolation threshold concentration. At this composition, according to Bunde et al. [21], the conductivity is governed by ion percolating paths across the sample. the formation of a space charge layer at the crystal-glass interface is equivalent to that of composite systems with two ionically conducting phases, MX/MX′ [22].

Figure 4 shows the variation of conductivity as a function of sintering temperature. The conductivity increases continuously with increase in the sintering temperature. The sintering temperature, however, is restricted to 798 K because the pellet deforms beyond this temperature. It is worth mentioning here that, as the concentration of the Na^+ glass increases, the deformation of the pellet occurs at relatively lower temperatures.

During sintering above T_g, the glass transforms to a semi-molten state and flows across the grains (capillary action) of the host Na_2CO_3 matrix, thereby filling the pores present therein. On cooling the pellet, the glass glues the grains together. The higher the sintering temperature, the more liquid the glass. Consequently, the surface interactions at the crystal-glass interface are expected to be more effective, thereby increasing the charge carrier (interstitial and vacancies) density in the space charge layer. A highly disordered space charge layer facilitates the ionic mobility. Hence, the conductivity increases with increases in the sintering temperature.

Figure 5 shows a typical variation of sensor emf as a parametric function of the CO_2 partial pressure on switching between 500 ppm to 1%, at a fixed oxygen partial pressure (21%) and remaining argon carrier gas. The cell emf exponentially increases/decreases upon changes in the test gas concentration and attains a steady state value. Further, the saturation in the emf is seen to be same in each cycle, confirming the perfect reversibility of the sensor. The time required to attain 90% of the saturation value is defined as the sensor response time. The response time of about 60 s observed for the present sensor is less than that reported by Sadaoka et al. [23]. The variation of cell emf with time (at a fixed CO_2 gas

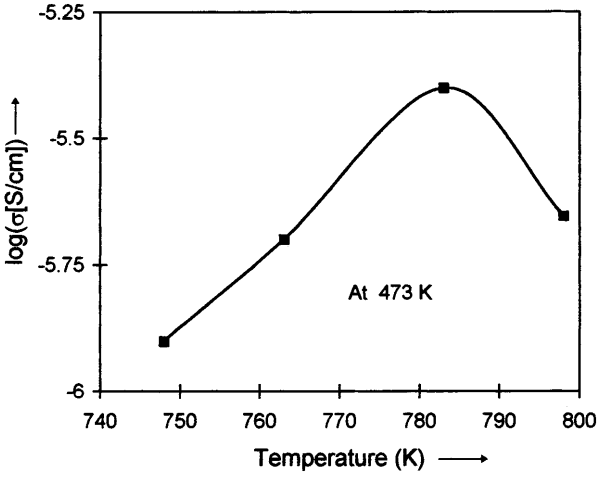

Fig. 4 Variation of $\log(\sigma)$ with sintering temperature

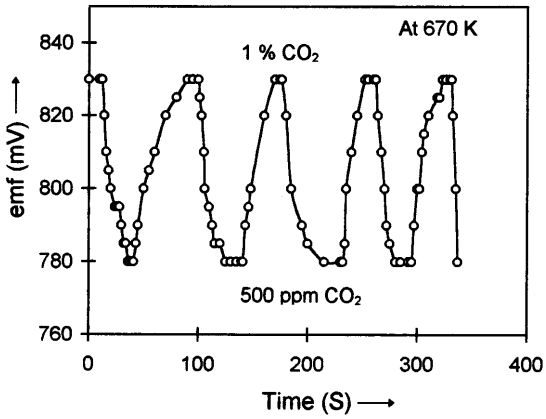

Fig. 5 Variation of sensor emf with time after change in CO_2 partial pressure

partial pressure and temperature) for sensor S_p (after the fifth thermal cycle) and sensor S_c (after second thermal cycle) is depicted in Fig. 6 a and b, respectively. Evidently, S_p degrades after only the second cycle of cooling and heating (Fig. 6b). On the other hand, S_c shows a stable performance even after the seventh thermal cycle (Fig. 6a). A critical microstructural analysis (Fig. 7 a and b) reveals that the sensor S_p develops micro-cracks during the thermal cycling. Sensor S_c (using a glass-bonded composite as the electrolyte), however, remains intact after the seventh thermal cycle.

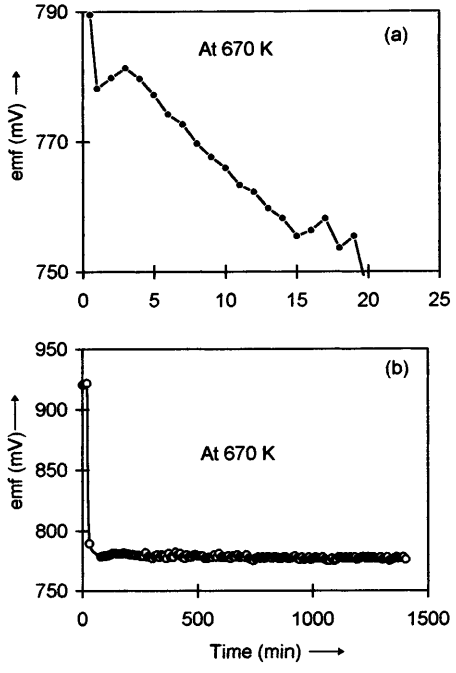

Fig. 6 Variation of emf with time at a fixed 100 ppm CO_2 partial pressure for sensors **a** S_p (pure Na_2CO_3, after second thermal cycle) and **b** S_c (composite solid electrolyte, after seventh thermal cycle)

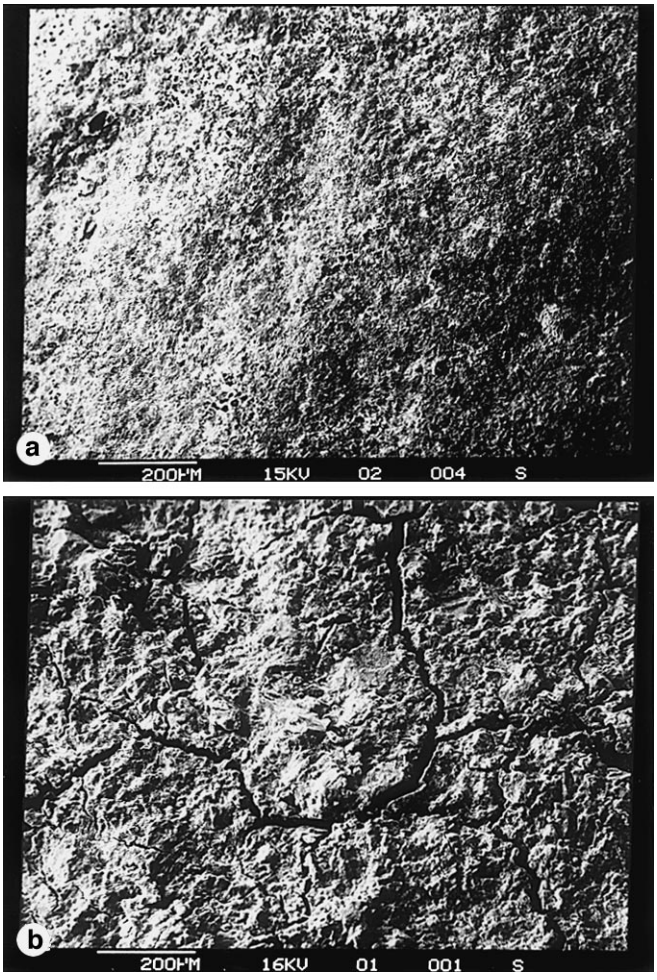

Fig. 7 Microstructures of sensor **a** S_c and **b** S_p

Conclusions

The dispersion of $[40Na_2O{:}50SiO_2{:}10B_2O_3]$ glass in a polycrystalline Na_2CO_3 matrix not only enhances the ionic conductivity of pure Na_2CO_3 but also improves the mechanical integrity and sinterability, leading to better performance and imperviousness to thermal shocks. The liquid phase sintering technique should provide a new route for the development of composite solid electrolytes useful for solid state gas sensors.

Acknowledgement The authors are thankful to DST, New Delhi, for providing the financial support to carry out this work.

References

1. Power RM, Mitof SP (1978) In: Hegenmuller P, Van V (eds) Solid electrolytes, Academic Press, New York, Chapter 9
2. Saito Y, Maruyama T, Matsumoto Y, Kobayashi K, Yano Y (1984) Solid State Ionics 14: 273
3. Singh K, Bhoga SS (1990) J Electrochem Soc 137: 1970
4. Gauthier M (1979) J Electrochem Soc 124: 1584

5. Hotzel G, Weppner W (1987) Sensors Actuators 12: 449
6. Saito Y, Maruyama T (1988) Solid State Ionics 28–30: 1644
7. Maier J, Warhus U (1986) J Chem Thermodyn 18: 309
8. Ishihara Y, Kometani K, Hashida M, Takita V (1991) J Electrochem Soc 138: 173
9. Ishiguro Y, Nagawa Y, Futata H (1986) Proc. 2nd international meeting on chemical sensors, France. Bordeaux p 719
10. Shimizu Y, Kamesi K, Egashira M (1989) J Electrochem Soc 136: 225
11. Ogata T (1986) J Mater Sci Lett 5: 285
12. Maruyama T, Sasaki S, Saito Y (1987) Solid State Ionics 23: 107
13. Gandhi PR, Salodkar RV, Singh K (1990) Ferroelectrics 102: 45
14. Singh K, Bhoga SS (1995) Ceylon Sci 2/1: 35
15. Wagner C (1957) Proc. Int. committee of electrochemical thermodynamics and kinetics, 7th meeting. Butterworths, London, p 61
16. Singh K, Bhoga SS (1997) Proc. 4th national seminar on physics and technology of sensors. Gujrat, India C23-1
17. Singh K, Bhoga SS (1990) J Mater Sci 25: 2520
18. Singh K, Bhoga SS (1998) Appl Phys A 67: 475
19. Singh K (1993) Solid State Ionics 66: 5
20. Maier J (1985) J Phys Chem Solids 46: 309
21. Bunde A, Dieterich W, Roman HE (1985) Phys Rev Lett 55: 5
22. Maier J, Ber Bunsenges Phys Chem 89: 355
23. Sadaoka Y, Matsuguchi M, Sakai Y, Manabe D (1993) J Mater Sci 28: 2035